of the adverse effects of PTX on gut immunity is thus an important research goal.

Gut-associated lymphoid tissue (GALT) has been considered a center of mucosal immunity because of its mass and function [12]. Anatomically, GALT is composed of organized lymphoid structures and diffusely distributed cell populations, such as intraepithelial (IE) and lamina propria (LP) lymphocytes. Organized GALT consists of Peyer patches (PP), which are regarded as the primary mucosal immune-inductive sites and sources of immunoglobulin (Ig) A-secreting cells. Once naïve lymphocytes have migrated into PP, they are sensitized and stimulated through interaction with dendritic cells and migrate to mesenteric lymph nodes, where they mature, proliferate, or both. After release into the thoracic duct, these lymphocytes are distributed by the vascular system to GALT effector (the LP and IE space) and extraintestinal sites.

This study examined whether PTX impairs gut immunity in mice. We examined the effects of a single intravenous dose of PTX on GALT (PP, LP, and IE) lymphocyte numbers, GALT cell phenotypes, and the secretory IgA concentration. Pathologic examination of the intestine also was performed.

Materials and Methods

Animals

The studies described herein conformed to the *Guidelines for the Care and Use of Laboratory Animals* established by the Animal Use and Care Committee of the National Defense Medical College. Male Institute of Cancer Research (ICR) mice, five weeks of age, were purchased from Japan SLC Inc (Hamamatsu, Japan). The ICR mouse is a standard strain for testing the toxicity, pharmacokinetics, and influences of drugs. In addition, many experimental studies focusing on the influences of nutrition on gut immunity in these animals have obtained results compatible with human clinical data. This strain has been used widely for evaluating gut immunity [13–15].

The mice were housed under controlled temperature and humidity conditions with a 12-h:12-h light:dark cycle. For acclimation, mice were fed commercial mouse chow (CE7, Clea, Japan) with water ad libitum for one week before protocol entry.

Surgical procedure

After the mice had been fasted overnight, they were given general anesthesia (ketamine 100 mg/kg and xylazine 10 mg/kg) and randomized into three groups: Control (n = 18), low-dose PTX (low PTX; n = 22), or high-dose PTX (high PTX; n = 24). All mice underwent implantation of silicon rubber catheters (0.3 mm inner and 0.5 mm outer diameter; Imamura Co., Tokyo, Japan) into the right jugular vein to assure intravenous (IV) administration of PTX. The proximal end of the catheter was tunneled subcutaneously over the spine and exited the tail at its midpoint. After these procedures, the mice were placed in individual metal metabolism cages and partially immobilized by tail restraint to protect the catheter during infusion. This technique is a well-established method that induces neither physical nor biochemical stress [16]. All procedures were performed aseptically. Catheterized mice were connected immediately to infusion pumps (TE331; Terumo, Tokyo, Japan) and received physiologic saline at 0.2 mL/h for 48 h with ad libitum access to chow and water.

Infusion protocol

The control group received a continuous IV infusion of physiologic saline at 0.2 mL/h throughout the study period with free access to chow and water (Fig. 1). On postoperative day 2, a single IV dose of PTX (Bristol Myers Squibb, Tokyo, Japan) was given to the low- (2 mg/kg) and high-dose (4 mg/kg) PTX groups. After the injection, the mice continued to receive saline at 0.2 mL/h throughout the study period with free access to chow and water.

At seven days after the injection, all mice were anesthetized (ketamine 100 mg/kg and xylazine 10 mg/kg) and exsanguinated by cardiac puncture. Complete blood cell counts were performed. Nasal and bronchoalveolar washings were obtained by lavage with 1 mL of phosphate-buffered saline. The entire small intestine was harvested and flushed with 20 mL of chilled Hank balanced salt solution (HBSS). The washings were stored in a −80°C freezer for later IgA analysis.

Peripheral blood-cell counts

Total numbers of leukocytes and the hemoglobin concentrations in the peripheral blood were measured with a hemocytometer (PCE-210; Erma Inc, Tokyo, Japan).

Cell isolation

Lymphocytes were isolated from the GALT using a modification of the method described by Li et al. [13]. The PP were examined as an inductive tissue for mucosal immunity.

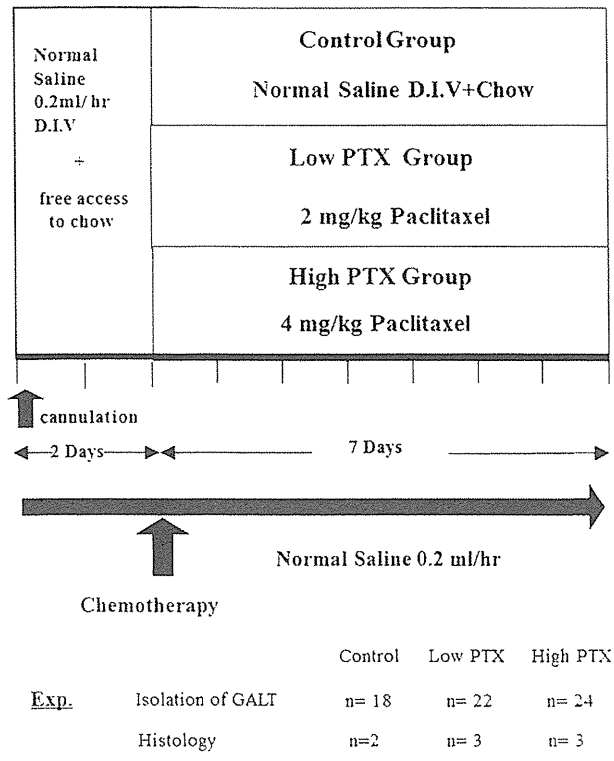

FIG. 1. Experimental protocol. All mice received a saline infusion with free access to chow and water. Mice were given low or high paclitaxel (PTX) doses intravenously at 2 mg/kg or 4 mg/kg, respectively. GALT = gut-associated lymphoid tissue.

Lymphocytes of the IE space and LP were chosen as gut mucosal immunity effector sites.

Peyer's Patches

The PP were excised from the serosal side of the intestine and teased apart. The fragments were treated with collagenase (40 U/mL; Sigma, St. Louis, MO) in Roswell Park Memorial Institute (RPMI) 1640 medium for 60 min at 37°C, with constant shaking. After collagenase digestion, the cell suspensions were passed through nylon filters.

Intraepithelial space and lamina propria

After PP excision, the intestine was turned inside out and cut into four segments. The segments were incubated with RPMI 1640 containing 5% fetal bovine serum (FBS), 1% glutamine, and a 1% antibiotic mixture (penicillin and streptomycin; GIBCO, Auckland, New Zealand), for 45 min at 37°C in a water shaker (150 rpm). Supernatant liquids containing released sloughed epithelial cells and IE lymphocytes were stored on ice. The remaining tissue pieces were incubated three times, 45 min each time, with RPMI 1640 containing collagenase (40 U/mL; Sigma), 5% FBS, glutamine, and the antibiotic mixture at 37°C at 150 rpm in a water shaker. Supernatant liquids containing LP cells from each of the incubations were pooled on ice. Supernatant liquids were filtered through a glass wool column. Suspensions were centrifuged, the pellets were resuspended in 40% Percoll (Pharmacia, Piscataway, NJ), and the cell suspensions were overlaid on 75% Percoll. After centrifugation for 20 min at 600 × *g* at 25°C, viable lymphocytes were recovered and washed in RPMI 1640. The lymphocytes were resuspended in RPMI 1640 with 5% FBS, 1% glutamine, and the 1% antibiotic mixture and then counted. This procedure yields a cell population that is 95%–100% viable by trypan blue exclusion.

Flow cytometry

Lymphocytes (1×10^5) isolated from PP, the IE space, and the LP were suspended in 50 mcL of HBSS containing fluorescein isothiocyanate (FITC) anti-mouse γδ T-cell receptor (TCR) (clone GL3; Caltag, Burlingame, CA) and phycoerythrin (PE)-conjugated antimouse βTCR (clone H57–597; Pharmingen, San Diego, CA) to identify γδTCR+ T and αβTCR+ T cells, respectively, or PE-anti-CD4 (clone CT-CD4; Caltag) and either FITC-anti-CD8α (clone CT-CD8a; Caltag) to identify the two T-cell subsets or FITC-anti-CD45R (B220; clone RA3–6B2; Caltag) to identify B cells. All antibodies were diluted to 1 mcg/mL in HBSS containing 1% FBS. Incubations were carried out for 30 min on ice. After staining, the cells were washed twice in HBSS/1% FBS and fixed in 1% paraformaldehyde. Flow cytometric analyses were performed on an Epics XL (Coulter, Inc., Hialeah, IL).

IgA quantification

Immunoglobulin A was measured in intestinal, nasal, and bronchoalveolar washings in a sandwich enzyme-linked immunosorbent assay using a polyclonal goat anti-mouse IgA (Sigma) to coat the plate, a purified mouse IgA (Zymed Laboratories, San Francisco, CA) as the standard, and a horseradish peroxidase–conjugated goat anti-mouse IgA (Sigma).

Histologic examination

To assess the influences of PTX on gut morphology, tissue sections of intestines collected from another set of mice (control: n = 2, low PTX: n = 3, high PTX: n = 3) were examined. The harvested intestine was cut into three sections, and each piece was fixed by immersion in 10% buffered formalin. For light microscopy, tissue samples were embedded in paraffin, sectioned, and stained with hematoxylin and eosin (H&E).

Statistical analysis

All data are expressed as the mean ± standard error of the mean for each group. Statistical significance was determined using analysis of variance (ANOVA) followed by the Fisher protected least-significant difference post-hoc test. Differences were considered significant at $p < 0.05$. All statistical calculations were performed with SPSS Software for Windows (SPSS, Inc., Chicago, IL).

Results

Body weight

There were no significant differences in body weight in the three groups at the beginning of the experiment (mean 32.1 ± 1.3 g [standard error] control; 31.5 ± 1.5 g low-PTX; 31.6 ± 1.4 g high-PTX).

Blood cell count

There were no significant differences in complete blood cell counts, including white blood cell counts and hemoglobin concentrations, among the three groups (Table 1).

Body weight change and food intake

We found no significant difference in body weight change or daily food intake among the three groups during the seven days after PTX injection (Fig. 2).

Total cell yields from GALT

The PP lymphocyte numbers were significantly lower in the high-PTX than in the control group (Fig. 3). The low-PTX group was midway between the control and high-PTX groups. The numbers of lymphocytes isolated from the IE and LP did not differ significantly among the three groups.

GALT phenotype

The PP and LP lymphocytes showed no significant differences in the percentages of αβTCR+, γδTCR+, CD4+, CD8+, or B220+ cells among the three groups (Tables 2–4). However, in the IE spaces, the percentages of CD4+ cells were significantly higher in the control group than in either the low- or the high-PTX group (Table 3). Absolute numbers of

TABLE 1. MEAN BLOOD CELL COUNTS ± STANDARD ERROR

	Control	*Low paclitaxel*	*High paclitaxel*
White blood cells (/mcL)	8,200 ± 1,100	7,500 ± 550	7,700 ± 1,000
Hemoglobin (g/dL)	12.9 ± 0.2	12.7 ± 0.2	12.7 ± 0.3

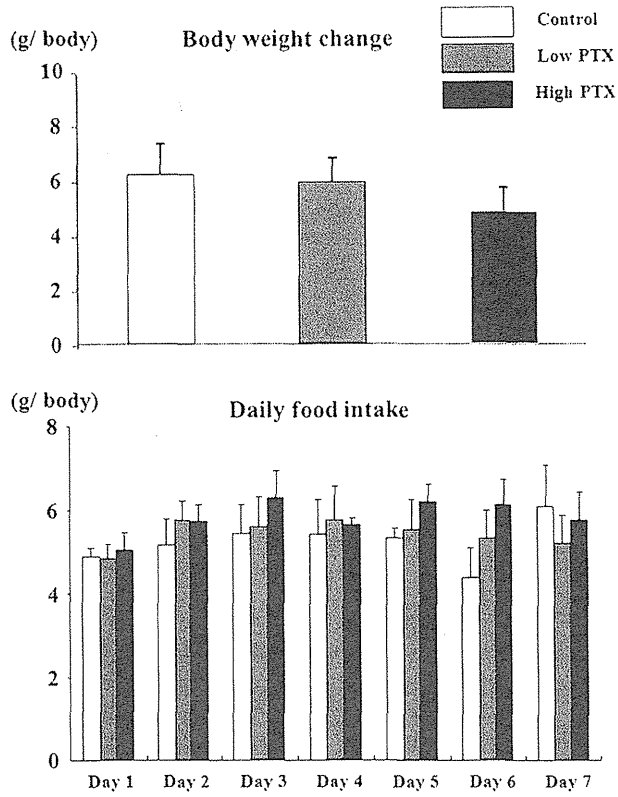

FIG. 2. Body weight changes and daily food intake. Values are means ± standard error. PTX = paclitaxel.

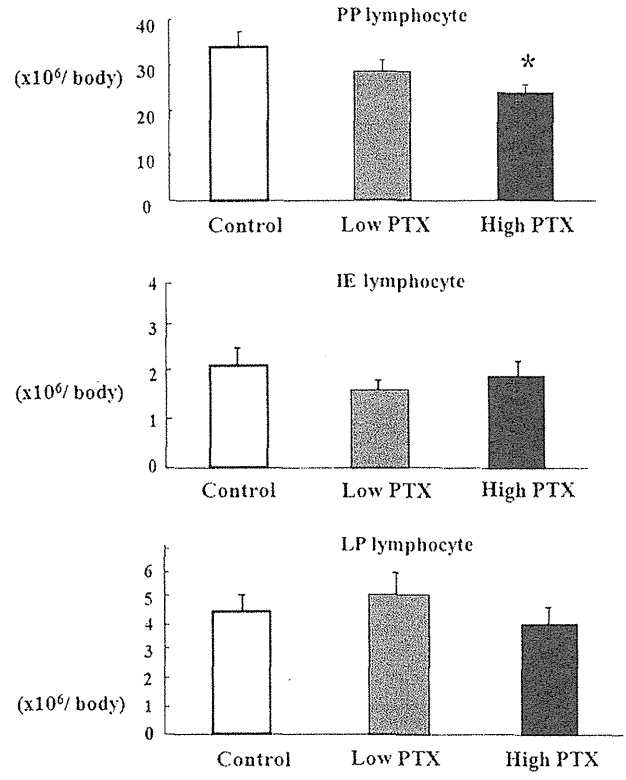

FIG. 3. Total cell yields from gut-associated lymphoid tissue (GALT). Values are means ± standard error. *$p < 0.05$ vs. control (analysis of variance). PTX = paclitaxel; PP = Peyer patches; IE = intraepithelial; LP = lamina propria.

TABLE 2. MEAN GUT-ASSOCIATED LYMPHOID TISSUE PHENOTYPE PERCENTAGES ± STANDARD ERROR IN PEYER PATCHES

	Control	*Low paclitaxel*	*High paclitaxel*
αβ	27.0 ± 1.1	25.3 ± 0.9	26.8 ± 0.5
γδ	0.7 ± 0.02	0.7 ± 0.02	0.6 ± 0.02
CD4	27.2 ± 1.0	23.8 ± 0.9	25.3 ± 0.5
CD8	1.9 ± 0.3	2.0 ± 0.2	2.2 ± 0.2
B220	44.1 ± 1.3	46.2 ± 1.1	46.4 ± 1.2

γδTCR+ and CD4+ cells in PP were significantly lower in the high-PTX than in the control group. In addition, there were significantly more CD4+ cells in the IE spaces in the control group than in either of the PTX groups (Fig. 4).

Secretory IgA concentration

There were no significant differences in intestinal IgA concentration among the three groups (Fig. 5). Nasal and respiratory tract IgA concentrations were significantly lower in the high-PTX than in the control group when we defined these concentrations as those of nasal plus bronchoalveolar washings. The low-PTX group was midway between the control and high-PTX groups in these measures, but the differences did not reach statistical significance.

Histopathologic changes

Figure 6 shows representative H&E staining of the distal portion of small-intestinal sections from the control, low-PTX, and high-PTX groups. In the high-PTX group, PP size was decreased, whereas the low-PTX group showed only minor changes (Fig. 6A–C). However, the histologic appearances of luminal structures such as villous height or mucosal thickness were similar in the three groups. In the proximal and middle portion of the small intestine, a similar finding was observed (Fig. 6D–F).

Discussion

The present study demonstrated the influence of PTX on GALT cell mass and function. A high dose of PTX reduced lymphocyte numbers at PP GALT inductive sites, with decreased absolute numbers of γδTCR+ and CD4+ cells, but did not influence total lymphocyte numbers in GALT effector sites. In association with the GALT mass reduction, nasal and respiratory tract IgA concentrations were decreased in the high-PTX group, whereas the IgA concentration in the

TABLE 3. MEAN GUT-ASSOCIATED LYMPHOID TISSUE PHENOTYPE PERCENTAGES ± STANDARD ERROR IN INTRAEPITHELIAL SPACES

	Control	*Low paclitaxel*	*High paclitaxel*
αβ	36.1 ± 0.5	37.5 ± 1.9	33.7 ± 2.1
γδ	9.9 ± 1.6	11.2 ± 3.0	11.9 ± 4.6
CD4	19.5 ± 2.3	11.2 ± 1.4[a]	10.9 ± 1.9[a]
CD8	32.8 ± 5.1	46.0 ± 8.1	39.5 ± 8.3
B220	10.5 ± 1.5	8.7 ± 1.5	7.5 ± 1.6

[a]$P < 0.05$ vs. control (analysis of variance).

TABLE 4. MEAN GUT-ASSOCIATED LYMPHOID TISSUE PHENOTYPE PERCENTAGES (±STANDARD ERROR) IN LAMINA PROPRIA

	Control	*Low paclitaxel*	*High paclitaxel*
αβ	26.1±2.1	24.7±3.3	21.3±2.0
γδ	6.0±0.9	7.0±0.9	5.8±1.3
CD4	17.5±2.3	14.7±2.3	13.1±2.4
CD8	14.6±1.6	15.3±1.4	12.0±0.8
B220	3.9±0.8	4.6±0.7	5.0±0.7

intestinal washings did not show significant differences among the three groups.

The absolute numbers of CD4+ cells in PP and IE spaces and of γδTCR+ cells in the PP were significantly higher in the control than in the high-PTX group. Reduction in absolute numbers of CD4+ and γδTCR+ cells in the PP as a result of PTX injection may impair systemic mucosal immunity. In fact, a reduction in CD4+ cells in GALT in the absence of enteral nutrition has been documented in association with impaired mucosal immunity [13,17]. In addition, intestinal γδ+ T lymphocytes are mainly involved in innate immunity and help to maintain mucosal homeostasis by participating in oral tolerance to food antigens and intestinal flora, in mucosal tissue repair, and in immunity to viral antigens and tumor cells [18–21]. Moreover, a recent study showed that activated human γδ T cells can serve as antigen-presenting cells and induce both Th- and Tc-cell-mediated responses [22]. New therapeutic

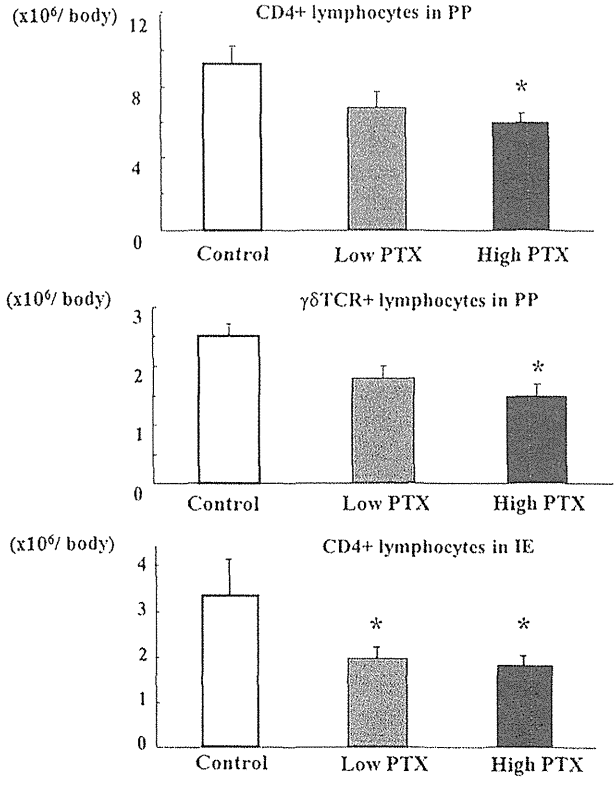

FIG. 4. Absolute numbers of $CD4^+$ lymphocytes in Peyer patches (PP) and intraepithelial (IE) spaces or γδ+ lymphocytes in PP. Values are means±standard error. *$p<0.05$ vs. control (analysis of variance) PTX=paclitaxel.

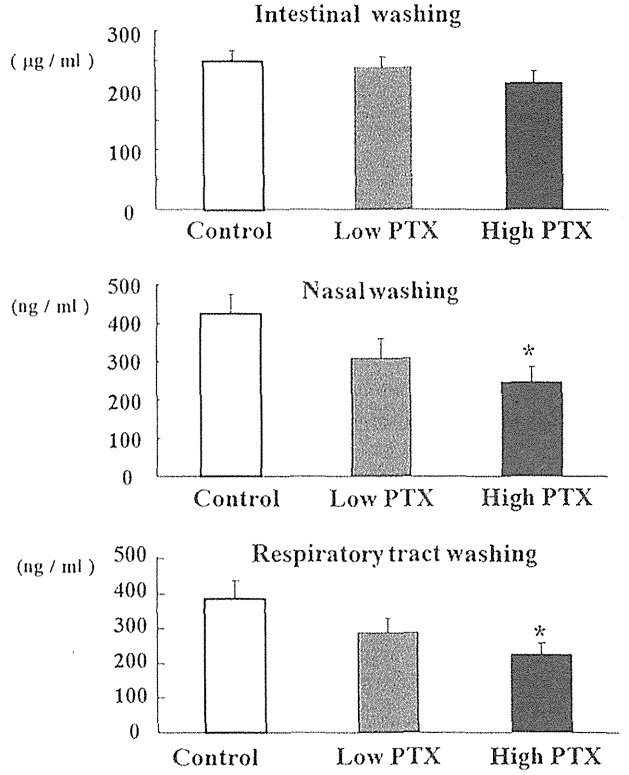

FIG. 5. Mean secretory IgA concentration±standard error. Respiratory tract washings=(nasal+bronchoalveolar washings)/2. *$P<0.05$ vs. control (analysis of variance). PTX=paclitaxel.

methods to increase these lymphocytes during chemotherapy are needed.

Although our present results do not elucidate the mechanisms underlying the decreased PP cell number in the high-PTX group, we can speculate about some possible mechanisms. One possibility involves the effects of PTX on microtubules and cell proliferation. Because PTX inhibits cell proliferation by stabilizing microtubules [11] and PP lymphocytes proliferate more than IE and LP lymphocytes, the influence of PTX on PP may have been greater than that on IE spaces and LP. To the contrary, we previously reported administration of 5-fluorouracil (5-FU), an inhibitor of thymidylate synthese, to reduce lymphocyte numbers in IE spaces and LP without marked changes in PP lymphocyte number [23]. Second, PTX may have lowered adhesion-molecule expression on the high endothelial venules of PP, leading to reduction of PP cell number, because PTX reportedly exerts inhibitory effects on endothelial-cell adhesion and migration [24]. In therapy for coronary artery disease, PTX drug-eluting stents prevent in-stent re-stenosis by inhibiting endothelial-cell adhesion and migration [25]. A previous study indicated that exposure to PTX downregulates the expressions of lymphocyte function-associated antigen (LFA)-1 and intercellular adhesion molecule (ICAM)-1 in mastocytomas [26]. In addition, colchicine, a drug that inhibits cell microtubules, inhibits CD54 expression by human umbilical-vein endothelial cells as well as LFA-1 expression by human T lymphocytes [27]. Therefore, the interaction between naïve lymphocytes and endothelial cells may be altered in response to PTX.

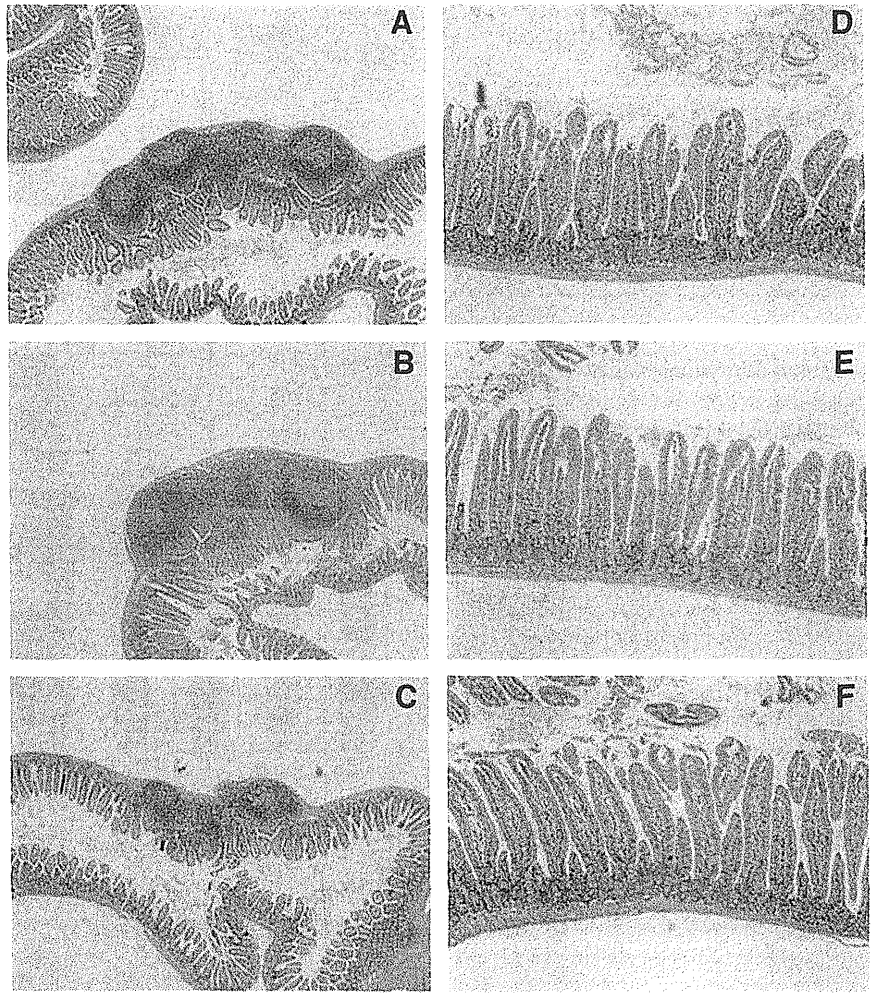

FIG. 6. Hematoxylin and eosin-stained sections of representative small intestinal tissues from control and low- and high-dose paclitaxel mice. Histopathologic changes are described in the text. Peyer patches from control (**A**), low-dose (**B**), and high-dose (**C**) mice. Small intestine from distal sites in the control (**D**), low-dose (**E**), and high-dose group (**F**). (Original magnification × 200 (A–C) and × 400 (D–F). Color image is available online at www.liebertpub.com/sur

Unexpectedly, the IgA concentration in small intestinal washings did not differ significantly among the three groups regardless of whether or not PP cell numbers were reduced. One possible reason may be the maintenance of LP number despite PTX treatment. The LP is the major gut mucosal effector site enriched with IgA-producing cells. Otherwise, polymeric immunoglobulin receptor (pIGR), produced by epithelial cells, might be preserved in the PTX group, as PTX treatment did not affect the gut epithelial layer in a histologic study [28]. The pIgR is a specialized transport protein for IgA, which affects the luminal IgA concentration. Nevertheless, a decrease in respiratory tract IgA concentration as a result of high-dose PTX may have been associated with reduced PP cell number and suggests impaired extraintestinal mucosal immunity.

Generally, administration of anticancer drugs reduces villous height and mucosal thickness, as reflected by the GI side effects of these drugs [29,30]. Taxanes induce unique histologic changes in the epithelium of the GI tract associated with cell necrosis [11]. However, the dose in this study did not cause gut morphologic changes. Previously, Kadota et al. reported no abnormal histologic findings in the jejunum or the ileum after intravenous administration of PTX to rats [31]. The doses given by Kadota et al. were much higher than those administered in the current study. Mason et al. examined the effect of PTX on the GI mucosa in a murine model, with injections of single doses of 10 and 40 mg/kg of PTX [32]. They demonstrated the appearance of the jejunal mucosa to be nearly normal at 24 h after PTX administration, whereas mitotically arrested cells could be seen in the proliferative zone at 3–4 h. Therefore, our gut morphology data are broadly consistent with the results from these previous studies.

Because chemotherapy is often associated with a variety of disturbances that can affect nutritional status profoundly, chemotherapy-induced malnutrition may reduce the secretory IgA response and GALT lymphocyte number. However, low- and high-PTX mice ate almost the same amount of chow as the control group, and body weight changes did not differ significantly among the three groups in the present study. In addition, blood cell counts showed no significant differences. Thus, we do not consider the GALT alterations observed in this study to be attributable to nutritional factors.

The present data suggest that during chemotherapy with PTX, special tactics aimed at preserving mucosal immunity may be needed. We demonstrated previously that

concomitant infusion of fish oil with 5-FU reverses 5-FU-induced GALT atrophy and normalize the respiratory tract IgA concentration [33]. Certain dietary compounds, especially probiotics and fiber, enhance intestinal secretory IgA production in healthy animals [34]. In addition, diets rich in flavonoids, such as cocoa and apple polyphenols, increase the γδ T cell population in GALT [35,36]. Supplements containing these immune-enhancing nutrients need to be tested as a possible strategy for avoiding PTX-induced impairment of mucosal immunity.

Based on pharmacologic information about PTX, the lethal dose (LD_{50}) for mice given intravenous injections is approximately 12 mg/kg. In our preliminary study, we examined the effects of intravenously administering 6, 4, and 2 mg/kg of PTX to mice. The body weights of the animals treated with 6 mg/kg had decreased markedly after seven days, whereas the other two groups showed no weight loss. Thus, 4 mg/kg and 2 mg/kg do not appear to cause malnutrition and were chosen for this study. In addition, these doses are relevant to clinical use, although the difference between mg/m^2 and mg/kg is a problem.

The current study has limitations. We performed a pilot study with a five-day time frame. However, neither the 2 mg/kg nor the 4 mg/kg dose of PTX produced deficits in gut immunity. Next, we extended the period to seven days and obtained the present data. We administered only a single dose of the drug, not repeated injection, as would be done in the clinical setting. Moreover, we observed GALT atrophy at only one time point; i.e., seven days after PTX injection. We recognize the importance of conducting a longitudinal study. Our future studies will focus on reducing the impacts of these limitations.

In conclusion, intravenous administration of high doses of PTX reduces PP lymphocyte numbers and the respiratory tract IgA concentration, whereas low-dose PTX has relatively minor effects. Because PTX has been considered to have relatively minor GI side effects, clinicians may not pay attention to gut function during chemotherapy with this drug. However, the present study raises the possibility of paclitaxel-related impairment of gut immunity, leading to a higher risk of respiratory tract infection. Careful dose selection and new therapies may be important for maintaining mucosal immunity during PTX chemotherapy.

Author Disclosure Statement

We received no financial or commercial sponsorship and no support from grants, organizations, or donations of equipment or drugs for this work.

References

1. Torres K, Horwitz SB. Mechanisms of Taxol-induced cell death are concentration dependent. Cancer Res 1998;58: 3620–3626.
2. Wu Y, Shen D, Chen Z, et al. Taxol induced apoptosis regulates amino acid transport in breast cancer cells. Apoptosis 2007;12:593–612.
3. Bishop JF, Dewar J, Toner GC, et al. Initial paclitaxel improves outcome compared with CMFP combination chemotherapy as front-line therapy in untreated metastatic breast cancer. Clin Oncol 1999;17:2355–2364.
4. Martín M, Rodríguez-Lescure A, Ruiz AJ, et al. Randomized phase 3 trial of fluorouracil, epirubicin, and cyclophosphamide alone or followed by paclitaxel for early breast cancer. J Natl Cancer Inst 2008;100:805–814.
5. Rowinsky EK, Donehower RC. Paclitaxel (Taxol). N Engl J Med 1995;332:1004–1014.
6. Rowinsky EK, Burke PJ, Karp JE, et al. Phase I and pharmacodynamic study of taxol in refractory adult acute leukemias. Cancer Res 1989;49:4640–4647.
7. Hurwitz CA, Relling MV, Weitman SD, et al. Phase I trial of paclitaxel in children with refractory solid tumors: A Pediatric Oncology Group study. J Clin Oncol 1993;11:2324–2329.
8. Daniele B, Rossi GB, Losito S, et al. Ischemic colitis associated with paclitaxel. J Clin Gastroenterol 2001;33:159–160.
9. Daniels JA, Gibson MK, Xu L, et al. Gastrointestinal tract epithelial changes associated with taxanes: Marker of drug toxicity versus effect. Am J Surg Pathol 2008;32:473–477.
10. Sheppard BC, Rutten MJ, Meichsner CL, et al. Effects of paclitaxel on the growth of normal, polyposis, and cancerous human colonic epithelial cells. Cancer 1999;85:1454–1464.
11. Hruban RH, Yardley JH, Donehower RC, et al. Taxol toxicity: Epithelial necrosis in the gastrointestinal tract associated with polymerized microtubule accumulation and mitotic arrest. Cancer 1989;63:1944–1950.
12. Kelsall B, Strober W. Gut-associated lymphoid tissue: Antigen handling and T-lymphocyte responses. In: Ogra PL, Mestecky J, Lamm ME, et al., editors. Mucosal Immunology. Second Edition. San Diego. Academic Press, 1999:293–317.
13. Li J, Kudsk KA, Gocinski B, et al. Effects of parenteral and enteral nutrition on gut-associated lymphoid tissue. J Trauma 1995;39:44–51.
14. Okamoto K, Fukatsu K, Ueno C, et al. T lymphocyte numbers in human gut associated lymphoid tissue are reduced without enteral nutrition. JPEN J Parenter Enteral Nutr 2005; 29:56–58.
15. Kang W, Kudsk KA. Is there evidence that the gut contributes to mucosal immunity in humans? JPEN J Parenter Enteral Nutr 2007;31:246–258.
16. Sitren HS, Heller PA, Bailey LB, et al. Total parenteral nutrition in the mouse: Development of a technique. JPEN J Parenter Enteral Nutr 1983;7:582–586.
17. King BK, Li J, Kudsk KA, et al. A temporal study of TPN-induced changes in gut-associated lymphoid tissue and mucosal immunity. Arch Surg 1997;132:1303–1309.
18. Hänninen A, Harrison LC. Gamma delta T cells as mediators of mucosal tolerance: The autoimmune diabetes model. Immunol Rev 2000;173:109–119.
19. Boismenu R. Function of intestinal γδ T cells. Immunol Res 2000;21:123–127.
20. Born WK, Jin N, Aydintug MK, et al. γδ T lymphocytes: Selectable cells within the innate system? J Clin Immunol 2007;27:133–144.
21. Born WK, Reardon CL, O'Brien RL, et al. The function of γδ T cells in innate immunity. Curr Opin Immunol 2006;18: 31–38.
22. Brandes M, Willimann K, Moser B, et al. Professional antigen-presentation function by human γδ T cells. Science 2005;309:264–268.
23. Nagayoshi H, Fukatsu K, Ueno C, et al. 5-Fluorouracil infusion reduces gut-associated lymphoid tissue cell number and mucosal immunoglobulin A levels. JPEN J Parenter Enteral Nutr 2005;29:395–400.
24. Li H, Zhang LJ, Chen BH et al. inhibitory effect of paclitaxel on endothelial cell adhesion and migration. Pharmacology 2010;85:136–145.

25. Davis HW, VandenBerg E, Reid MD, et al. Paclitaxel impairs endothelial cell adhesion but not cytokine-induced cellular adhesion molecule expression. Ann Vasc Surg 2005;19:398–406.
26. Zhao C, Morgan M, Haeryfar SM, et al. Exposure to paclitaxel or vinblastine down-regulates CD11a and CD54 expression by P815 mastocytoma cells and renders the tumor cells resistant to killing by nonspecific cytotoxic T lymphocytes induced with anti-CD3 antibody. Cancer Immunol Immunother 2003;52:185–193.
27. Perico N, Ostermann D, Bontempelli M, et al. Colchicine interferes with L-selectin and leukocyte function associated antigen-1 expression on human T lymphocytes and inhibits T cell activation. J Am Soc Nephrol 1996;7:594–560.
29. Hermsen JL, Sano Y, Kudsk KA. Food fight! Parenteral nutrition, enteral stimulation and gut-derived mucosal immunity. Langenbecks Arch Surg 2009;394:17–30.
29. Tsuji E, Hiki N, Nomura S et al Simultaneous onset of acute inflammatory response, sepsis-like symptoms and intestinal mucosal injury after cancer chemotherapy. Int J Cancer 2003;107:303–308.
30. Leblond J, Le Pessot F, Hubert-Buron A, et al. Chemotherapy-induced mucositis is associated with changes in proteolytic pathways. Exp Biol Med 2008;233:219–228.
31. Kadota T, Chikazawa H, Kondoh H. [Toxicity studies of paclitaxel (II): One-month intermittent intravenous toxicity in rats] (Jpn; English abstract). J Toxicol Sci 1994;19(Suppl 1):11–34.
32. Mason KA, Milas L, Peters LJ, et al. Effect of paclitaxel (taxol) alone and in combination with radiation on the gastrointestinal mucosa. Int J Radiat Oncol Biol Phys 1995;32: 1381–1389.
33. Fukatsu K, Nagayoshi H, Maeshima Y, et al. Fish oil infusion reverses 5-fluorouracil-induced impairments in mucosal immunity in mice. Clin Nutr 2008;27:269–275.
34. Vetrano S, Correale C, Borroni EM, et al. Colifagina, a novel preparation of 8 lysed bacteria ameliorates experimental colitis. Int J Immunopathol Pharmacol 2008;21:401–407.
35. Akiyama H, Sato Y, Watanabe T, et al. Dietary unripe apple polyphenol inhibits the development of food allergies in murine models. FEBS Lett 2005;579:4485–4491.
36. Ramiro-Puig E, Pérez-Cano FJ, Ramos-Romero S, et al. Intestinal immune system of young rats influenced by cocoa-enriched diet. J Nutr Biochem 2008;19:555–565.

Address correspondence to:
Dr. Tomoyuki Moriya
Department of Surgery
National Defense Medical College
3-2, Namiki, Tokorozawa
Saitama, Japan 359-8513

E-mail: tmoriya@ndmc.ac.jp

World J Surg
DOI 10.1007/s00268-014-2715-8

ORIGINAL SCIENTIFIC REPORT

Clinical Significance of Anatomical Variant of the Left Hepatic Artery for Perihilar Cholangiocarcinoma Applied to Right-Sided Hepatectomy

Hiroaki Shimizu · Isamu Hosokawa · Masayuki Ohtsuka · Atsushi Kato · Hideyuki Yoshitomi · Masaru Miyazaki

Abstract

Background Full understanding of the hilar anatomy is crucial for successful surgical resection of perihilar cholangiocarcinoma (PHC).

Methods The three-dimensional positional relationship between the left hepatic artery (LHA) and the umbilical portion of the left portal vein (UP) was evaluated using multidetector-row computed tomography (CT) in 58 consecutive patients who underwent right-sided hepatectomy for Bismuth–Corlette IIIa or IV tumors. The positional relationship of the LHA related to UP was classified into the following three types: L-UP type, LHA runs into the left lateral section (LLS) from the left caudal side of the UP; R-UP type, LHA runs into the LLS from the right cranial side of the UP; and combined type, one branch of the LHA runs into the LLS from the right cranial side of the UP, and the other from the left caudal side of the UP.

Results L-UP-type LHA was observed in 53 cases (91.4 %), R-UP type in three cases (5.2 %), and combined type in two cases (3.4 %). No cancer involvement of the LHA was seen in any cases with L-UP type. In one case with R-UP type (one of three; 33.3 %) and one case with combined type (one of two, 50 %), cancer invasion to the LHA was observed at the right side of the UP, requiring combined resection of the involved LHA.

Conclusions R-UP-type LHA running just along the left hepatic duct may be easily involved by right-side predominant PHC when extending to the left hepatic duct. Hepatobiliary surgeons should recognize this anatomical variant and carefully evaluate the running courses of LHA to successfully perform R0 resection in right-sided hepatectomy for PHC.

Introduction

Preoperative recognition of the branching pattern and running course of the hepatic artery is essential for safe hepatobiliary surgery [1, 2]. Furthermore, three-dimensional (3D) anatomical evaluation of portal triad structures at the hepatic hilus is not only helpful in surgical orientation, but also crucial to achieve curative resection in patients with perihilar cholangiocarcinoma (PHC). With recent technical advances in diagnostic imaging, multidetector-row computed tomography (MDCT) allows recognition of the detailed branching pattern and running course of the hepatic artery without performing angiography [3]. Furthermore, we can easily evaluate the 3D relationship of the portal vein and hepatic artery with a workstation using 3D image analysis software [4]. The clinical significance of the 3D relationship of the right posterior sectional duct or right posterior hepatic artery (RPHA) in relation to the right portal vein (PV) has been reported for patients with PHC undergoing left-sided hepatectomy [5–7].

H. Shimizu (✉) · I. Hosokawa · M. Ohtsuka · A. Kato · H. Yoshitomi · M. Miyazaki
Department of General Surgery, Chiba University Graduate School of Medicine, 1-8-1 Inohana, Chuo-Ku, Chiba 260-8677, Japan
e-mail: h-shimizu@faculty.chiba-u.jp

Published online: 15 August 2014

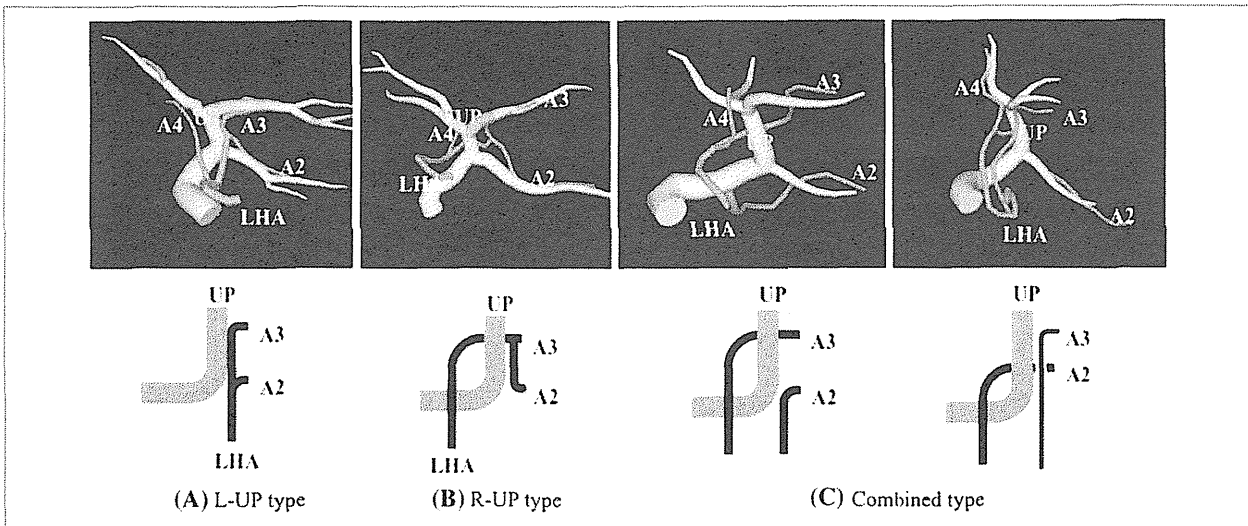

Fig. 1 Classification of the left hepatic artery according to the positional relationship to the umbilical portion of the left portal vein. Three-dimensional images of the structures based on data from MDCT, showing the three types of the LHA. **a** L-UP type: LHA runs into the LLS from the left caudal side of the UP; **b** R-UP type: LHA runs into the LLS from the right cranial side of the UP; **c** combined type: one branch of the LHA runs into the LLS from the right cranial side of the UP, and the other from the left caudal side of the UP. *LHA* left hepatic artery, *LLS* left lateral section, *MDCT* multidetector-row computed tomography, *UP* umbilical portion of the left portal vein

Hepatic arteries running to the left hemiliver are the laterosuperior segmental artery (A2), the lateroinferior segmental artery (A3), and the left medial segmental artery (A4). In this study, arteries feeding the left lateral segment (LLS) (segments II and III) were defined as the left hepatic artery (LHA). The LHA usually runs into the LLS from the left caudal side of the umbilical portion (UP) of the left PV (L-UP type), but occasionally runs into the LLS from the right cranial side of the UP (R-UP type), which courses just along the left hepatic duct.

In this study, we investigated the 3D positional relationships between the LHA and UP using MDCT and a workstation for 3D imaging to clarify the influence of this variation on clinicopathological outcomes in 58 consecutive patients who underwent right-sided hepatectomy for Bismuth–Corlette (B–C) IIIa or IV tumors [8] at our institution.

Patients and methods

Patients and surgical procedure

MDCT and clinicopathological data were retrospectively reviewed in 58 consecutive patients who underwent right-sided hepatectomy extending segment I with extrahepatic bile duct resection for PHC at the Department of General Surgery, Chiba University Hospital between January 2008 and July 2013. The 58 cases comprised 38 cases with B–C type IIIa tumor and 20 cases with B–C type IV tumor with right-side predominance. Right hemihepatectomy (RH) was applied for B–C type IIIa tumors ($n = 38$), and also for B–C type IV tumors ($n = 15$) when tumor extension to the left medial segmental branch (B4) was limited to near its confluence. In RH, the bile duct was divided just at the right side of the UP after completing liver resection. The B4 branch was divided first at the ventral side of the umbilical fissure, then left hepatic duct at its dorsal side, separately, resulting in two orifices of the B4 and left hepatic duct. Meanwhile, right trisectionectomy (RT) was indicated ($n = 5$) when B–C type IV tumors extended close to the umbilical fissure and/or extended to the peripheral portion of the B4. However, when B–C type IV tumor with right-side predominance extended beyond the right side of the UP, the tumor was considered as unresectable.

Classifications of LHA according to the positional relationship to the UP

In this study, arteries feeding the LLS (segments II and III) were defined as the LHA. LHA was then classified into the following three types according to the positional relationship to the UP: L-UP type, LHA runs into the LLS from the left caudal side of the UP; R-UP type, LHA runs into the LLS from the right cranial side of the UP, and combined type, one branch of the LHA runs into the LLS from the right cranial side of the UP, and the other from the left caudal side of the UP (Fig. 1).

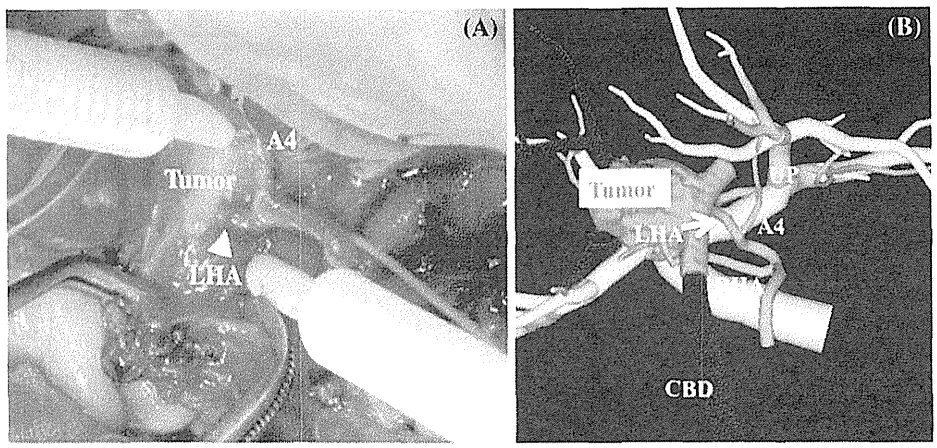

Fig. 2 Operative photograph (**a**) and three-dimensional image (**b**) of hilar structures based on data from MDCT in a case with the R-UP type of left hepatic artery. The LHA (*arrow*) shows involvement by the biliary tumor at the right side of the umbilical portion of the left portal vein. *A4* the left medial segmental artery, *CBD* common bile duct, *LHA* left hepatic artery, *MDCT* multidetector-row computed tomography, *PV* portal vein, *RHA* right hepatic artery, *UP* umbilical portion of the left portal vein

MDCT and workstation

All MDCT examinations were performed using a scanner with 64 rows of detectors (Acquisition One or 64; Toshiba Medical Systems, Tokyo, Japan). The slice thickness was 5 mm, and table feed was 5 mm. After obtaining a series of scans throughout the liver and biliary tree, each patient was injected with 110–150 ml of nonionic contrast material with an iodine content of 300 mg/ml at a rate of 3.5 ml/s with a power injector (Nemoto Kyorindo Co., Ltd., Tokyo, Japan). The bolus tracking method was used to scan each patient. The trigger threshold level was set at 200 Hounsfield units at the level of the descending aorta. The second, third, and fourth helical scans were then performed during the early hepatic arterial, late hepatic arterial, and equilibrium phases 5, 20, and 50 s after the trigger, respectively. For 3D image analysis using software (Synapse Vincent; Fuji Film, Co., Tokyo, Japan), MDCT scan data were transferred to a workstation. Structures of the liver, PV, and HA were extracted and 3D images of the structures were then constructed. These images could be rotated horizontally or vertically for evaluation of the positional relationships between the LHA and UP.

Results

In all of the 58 cases with right-sided hepatectomy, L-UP-type LHA was observed in 53 cases (91.4 %), and R-UP type was seen in three cases (5.2 %), as shown in Table 1. Combined type LHA was found in two cases (3.4 %); in one case, A3 entered segment III from the right cranial side of the UP, whereas A2 entered segment II from the left caudal side of the UP, while in the other case, only the inferior branch of A3 showed an R-UP course. Among all 58 cases, the LHA was originated from left gastric artery (replaced LHA) in four cases. Interestingly, the course to the LLS in all four cases was L-UP type. It is also noted that in all three cases with R-UP type, the A4 branch was originated from the R-UP type LHA at the right side of the UP.

Cancer involvement of the LHA was not found in any cases with L-UP-type LHA (Table 1). However, in one case with R-UP type LHA, the LHA was obviously involved at the right side of the UP (Fig. 2), but the confluence of the left lateral superior segmental duct (B2) and left lateral inferior segmental duct (B3) had not been invaded by tumor. Combined LHA resection was therefore performed for R0 resection during RH with PV resection and reconstruction, but LHA reconstruction could not be performed due to the technical difficulty. As a result, only the A4 branch was preserved. The intrahepatic duct was divided at the right side of the UP, resulting in two orifices of the B4 and left hepatic duct (B2 + B3) on the resected surface of the liver. The two bilioenteric anastomoses were then performed. Histopathological findings showed negative margins at both stumps of the B4 and the left hepatic (B2 + B3) ducts. Resected LHA showed histological invasion to the adventitia of this artery. Although R0 resection could be achieved in this case, bilioenteric anastomotic leakage occurred early after surgery, and sepsis resulting from an intra-abdominal abscess subsequently developed. After percutaneous abscess drainage, the patient recovered and was discharged from the hospital 39 days after surgery. In addition, in one patient with

Table 1 Relation between running course of left hepatic artery and cancer involvement of the LHA in 58 cases of right-sided hepatectomy for perihilar cholangiocarcinoma

	L-UP type	R-UP type	Combined type
Total (n = 58)	53 (91.8)	3 (5.2)	2 (3.4)
Operative procedures			
Right hemihepatectomy	48	3	2
Right trisectionectomy	5	0	0
Cancer involvement of LHA			
(+)	0 (0)	1 (33.3)	1 (50)
(−)	53	2	1

Data are presented as n (%)

LHA left hepatic artery, *L-UP* left hepatic artery runs into the left lateral section from the left caudal side of the umbilical portion of the left portal vein, *R-UP* LHA runs into the left lateral section from the right cranial side of the umbilical portion of the left portal vein

combined-type LHA, cancer involvement of the A3 branch with an R-UP course was found intraoperatively, and this variant artery was sacrificed to achieve R0 resection during RH. The intrahepatic duct was divided at the right side of the UP, resulting in two orifices of the B4 and left hepatic duct. In this case, no preoperative diagnosis of combined-type LHA was made. Fortunately, the postoperative course was largely uneventful with the exception of minor bilioenteric anastomotic leakage. According to the histopathological findings, both stumps of the B4 and the left hepatic duct were positive with cancer in situ, showing R1 resection.

Discussion

In surgical resection for PHC, hemihepatectomy extending to segment I with extrahepatic bile duct resection has been recognized as a standard surgical procedure [9, 10]. More aggressive surgical approaches, such as left trisectionectomy or RT combined with PV and/or HA resection and reconstruction have also often been performed in specialized centers [11–15]. At the same time, recent technical advances in diagnostic imaging, particularly MDCT and the use of workstations for 3D imaging, allow detailed evaluation not only of tumor extension into the bile duct, but also of the 3D relationships between bile duct, HA, and PV at the hepatic hilus in patients with PHC [16]. Previously, the clinical significance of the running course of the RPHA in relation to the right PV has been reported in cases of left-sided hepatectomy for PHC [6, 17]. Yoshioka et al. [6] clearly demonstrated that the supraportal variant of RPHA was not unusual, with an incidence of 20.4 %. Furthermore, careful dissection of the supraportal RPHA from the right hepatic duct is required to avoid injuring this variant artery during left-sided hepatectomies, particularly left trisectionectomy, because the artery runs just beneath the right hepatic duct.

Previous studies [16, 18, 19] have shown detailed anatomical variations of the left hepatic artery for hepatobiliary and transplant surgeries. The present study investigated the 3D positional relationship between the LHA and UP in 58 patients with PHC who underwent right-sided hepatectomy. We classified the LHA into three types (L-UP type, R-UP type, and combined type) according to its running course, and clearly demonstrated that L-UP-type LHA represented the normal running course of this artery, while other types, including R-UP and combined types, were anatomical variants with a total incidence of 8.7 %. Furthermore, cancer invasion to the variant LHA running into the LLS from the right cranial side of the UP was found in two of five cases (40 %). Conversely, cancer invasion to the L-UP-type LHA (n = 53) was not found in any cases. Overall, in the total of 58 cases, LHA involvement in patients with B–C type IIIa or IV tumors was extremely rare (2 of 58 patients, 3.4 %), but our findings strongly suggest that the running course of the LHA may influence surgical curability by itself in right-sided hepatectomy for PHC. That is, as R-UP-type LHA runs just along the left hepatic duct, this variant artery may be easily involved by right-side predominant PHC when extending to the left hepatic duct. Boudjema et al. [20] recently reported that when the confluence of B2 and B3 ducts was free of tumor, the LHA was never involved by the tumor and the tumor was always eventually resectable. Their conclusion is correct when the running course of LHA is the normal L-UP type, but R-UP-type variants of LHA carry a possibility of tumor involvement, albeit extremely rare.

In our series, combined resection of involved variant LHA was performed in two cases to achieve R0 resection during RH. However, from a technical perspective, reconstruction of the resected LHA variant at this peripheral level was much more difficult than that of the RHA. Generally, interruption of arterial flow to the remnant liver can cause serious postoperative complications related to biliary ischemia, including disruption of the bilioenteric anastomosis and liver abscess [21]. Occurrence of these complications after major hepatectomy may lead to a high risk of postoperative mortality [22, 23]. The LHA flow must therefore be maintained in cases with right-sided hepatectomy, particularly RT without exception. Furthermore, the R-UP variant might be mistaken for A4 at the right side of the UP and divided when performing RT because its running course looks like the A4. In addition, R-UP-type LHA enters the LLS just between the stump of the bile duct and UP. Greatest care is required during

bilioenteric anastomosis, as well as dissection of this variant artery from the left hepatic duct.

Conclusion

Although the R-UP variant of LHA was uncommon, with an incidence of 8.7 %, hepatobiliary surgeons should recognize this anatomical variant, and carefully evaluate the running course of the LHA in relation to the UP to successfully perform R0 resection and also to avoid postoperative complications when planning right-sided hepatectomy for PHC.

References

1. Hiatt JR, Gabbay J, Busuttil RW (1994) Surgical anatomy of the hepatic arteries in 1,000 cases. Ann Surg 220:50–52
2. Song SY, Chung JW, Yin YH et al (2010) Celiac axis and common hepatic artery variations in 5,002 patients: systematic analysis with spiral CT and DSA. Radiology 255:278–288
3. Sakai H, Okuda K, Yasunaga M et al (2005) Reliability of hepatic artery configuration in 3D CT angiography compared with conventional angiography: special reference to living-related liver transplant donors. Transpl Int 18(5):499–505
4. Endo I, Shimada H, Sugita M et al (2007) Role of three-dimensional imaging in operative planning for hilar cholangiocarcinoma. Surgery 142:666–675
5. Shimizu H, Sawada S, Kimura F et al (2009) Clinical significance of biliary vascular anatomy of the right liver for hilar cholangiocarcinoma applied to left hemihepatectomy. Ann Surg 49:435–439
6. Yoshioka Y, Ebata T, Yokoyama Y et al (2011) Supraportal right posterior hepatic artery: an anatomic trap in hepatobiliary and transplant surgery. World J Surg 35:1340–1344. doi:10.1007/s00268-011-1075-x
7. Ozden I, Kamiya J, Nagino M et al (2002) Clinicoanatomical study on the infraportal bile ducts of segment 3. World J Surg 26:1441–1445. doi:10.1007/s00268-002-6544-9
8. Bismuth H (1982) Surgical anatomy and anatomical surgery of the liver. World J Surg 6:3–9. doi:10.1007/BF01656368
9. Nagino M, Ebata T, Yokoyama Y et al (2013) Evolution of surgical treatment for perihilar cholangiocarcinoma: a single-center 34-year review of 574 consecutive resections. Ann Surg 258:129–140
10. Shimizu H, Kimura F, Yoshidome H et al (2010) Aggressive surgical resection for hilar cholangiocarcinoma of the left-sided predominance: radicality and safety of left-sided hepatectomy. Ann Surg 251:281–286
11. Natsume S, Ebata T, Yokoyama Y et al (2012) Clinical significance of left trisectionectomy for perihilar cholangiocarcinoma: an appraisal and comparison with left hepatectomy. Ann Surg 255:754–762
12. Hosokawa I, Shimizu H, Yoshidome H et al (2014) Surgical strategy for hilar cholangiocarcinoma of the left-side predominance: current role of left trisectionectomy. Ann Surg 259(6):1178–1185
13. Nagino M, Kamiya J, Arai T et al (2006) "Anatomic" right hepatic trisectionectomy (extended right hepatectomy) with caudate lobectomy for hilar cholangiocarcinoma. Ann Surg 243:28–32
14. Neuhaus P, Thelen A, Jonas S et al (2012) Oncological superiority of hilar en bloc resection for the treatment of hilar cholangiocarcinoma. Ann Surg Oncol 19:1602–1608
15. Machado MA, Makdissi FF, Surjan RC (2012) Right trisectionectomy with principal en bloc portal vein resection for right-sided hilar cholangiocarcinoma: no-touch technique. Ann Surg Oncol 19:1324–1325
16. Ibukuro K, Takeguchi T, Fukuda H et al (2013) Spatial relationship between the hepatic artery and portal vein based on the fusion image of CT angiography and CT arterial portography: the left hemiliver. AJR 200:1160–1166
17. Uesaka K (2012) Left hepatectomy or left trisectionectomy with resection of the caudate lobe and extrahepatic bile duct for hilar cholangiocarcinoma (with video). J Hepatobiliary Pancreat Sci 19:195–202
18. Seda-Neto J, Godoy AL, Carone E et al (2008) Left lateral segmentectomy for pediatric live-donor liver transplantation: special attention to segment IV complications. Transplantation 86:697–701
19. Hirano S, Kondo S, Tanaka E et al (2008) Safety of combined resection of the middle hepatic artery in right hemihepatectomy for hilar biliary malignancy. J Hepatobiliary Pancreat Sci 16:796–801
20. Boudjema K, Sulpice L, Garnier S et al (2013) A simple system to the predict perihilar cholangiocarcinoma resectability. J Gastrointest Surg 17:1247–1256
21. Suda K, Ohtsuka M, Ambiru S et al (2009) Risk factors of liver dysfunction after extended hepatic resection in biliary tract malignancies. Am J Surg 197:752–758
22. Miyazaki M, Kato A, Ito H et al (2007) Combined vascular resection in operative resection for hilar cholangiocarcinoma: does it work or not? Surgery 141:581–588
23. Nagino M, Nimura Y, Nishio H et al (2010) Hepatectomy with simultaneous resection of the portal vein and hepatic artery for advanced perihilar cholangiocarcinoma: an audit of 50 consecutive cases. Ann Surg 252:115–123

Current Organ Topics:

Section Leader: 宮崎 勝
千葉大学大学院医学研究院 臓器制御外科学

Liver, Pancreas, Biliary Tract Cancer
肝・胆・膵 癌

〔*Jpn J Cancer Chemother* 41(10): 1207-1208, *October*, 2014〕

総括

肝胆道膵癌において，遠隔転移のない局所進行癌に対しては，外科切除が唯一の根治性を得られる可能性がある治療方法である。しかし，しばしば肝胆道膵の癌の診断時には，その解剖学的臓器特異性より周囲の大血管への癌浸潤を認めるため，外科切除が困難な場合が少なくない。肝癌においては，背側に下大静脈および肝静脈が位置し，肝門部においては門脈・肝動脈が錯綜している。胆道癌においても，しばしば門脈・肝動脈浸潤を診断時に認めることが多く，その切除が極めて困難となる。また膵癌においても，門脈・肝動脈さらには上腸間膜動脈への癌浸潤が外科切除可否の大きなポイントとなることが多い。そのような大血管浸潤を伴った局所進行肝胆道膵癌において，血管合併切除を伴った外科切除で安全性を担保しつつ，surgical margin を確保した根治的切除を行い得られることにより，外科切除の適応は大きく拡大される。近年，このような肝胆道膵癌に対する血管合併切除の進展が飛躍的に向上してきている。またその結果，外科切除の恩恵に浴する患者も増加してきており，長期の予後にも徐々にその効果が反映されてきている。

肝癌においては，肝細胞癌では血管浸潤を来すことはまれで，血管内への腫瘍栓の進展が門脈および肝静脈・下大静脈に認められる際に，その外科切除においては血行遮断および血管再建が問題となる。多くの肝細胞癌の血管内腫瘍栓の進展では，直接血管壁に広範な浸潤をみることは少なく，腫瘍栓の摘除のみで血管合併切除を要することはまれである。しかし，下大静脈や門脈本幹を切開して腫瘍栓摘除を行うためには，total hepatic vascular exclusion などの血行遮断法を用いて大量出血および空気塞栓の予防を図る必要がある。血管合併切除を要する肝癌は，肝内胆管癌および転移性肝癌といった腺癌系の腫瘍で問題となる。下大静脈・肝静脈への浸潤を認める場合には，下大静脈再建および肝静脈再建が必要な場合があり，その再建には自家静脈グラフトおよびリング付き合成血管を用いる場合が多い。門脈再建も要する際には，自家静脈グラフトを用いると有益である。

胆道癌の局所進行例では，しばしば肝門部において門脈および肝動脈への癌浸潤を認め，その外科切除に血管合併切除を要する場合が少なくない。肝門部領域の胆道癌では，多くは右側あるいは左側肝切除を要するので，血行再建は残存肝領域への流入血管の再建ということになる。その際にしばしば問題となるのは残存肝への血流遮断であり，極力阻血時間を短くすることが術後の肝不全の防止には大切である。そのためには，血管再建手技は極めて重要なポイントとなる。術後の狭窄や血栓形成の防止も手術手技が重要となる。肝動脈再建を要した際には術後のヘパリン投与は必須であるが，門脈および下大静脈再建においては必ずしも抗凝固療法の意義は明確でない。

膵癌では，多くは膵頭部癌門脈浸潤においてその合併切除再建が必要となる。特に，上腸間膜静脈の末梢への癌浸潤が広範で門脈枝の再建を要するような場合に，その切除再建は工夫を要する。門脈切除長が長い場合には，自家静脈グラフトを用いての再建を行う必要があり，10～15%程度の門脈再建においてその必要性が認められる。

再建用に用いる自家静脈グラフトとして，これまで様々なものが用いられ報告されている。内外腸骨静脈，頸静脈および左腎静脈がこれまで多く報告されてきている。左腎静脈は1995年にわれわれが開発し報告してきたものであるが，他の自家静脈グラフトと異なり肝胆膵外科手術においては，同一術野からの採取が可能である点がその

Liver, Pancreas, Biliary Tract Cancer

Section Leader: Masaru Miyazaki
Dept. of General Surgery, Chiba University, Graduate School of Medicine

利点として強調される。また，門脈本幹の径ともよくマッチしており，その有用性は高く欧米でのその利用のMayo Clinicはじめ多くの報告が続いている。

肝胆膵癌の特に局所進行癌における血管合併切除術は，この領域の多くの癌で外科切除が唯一の根治治療法であることより，外科切除適応の拡大をなし得る極めて重要なポイントである。これからも外科医を中心として血管合併切除術の開発・発展がさらに継続されることで，より多くの患者に外科切除の恩恵を供与できるものと期待するところである。

膵癌診療ガイドライン2013の変更点

山口幸二*，日本膵臓学会膵癌診察ガイドライン改訂委員会

索引用語：ガイドライン，膵癌

1 はじめに

膵癌診療ガイドラインは2006年に初版が発刊され[1]，2009年に改訂され[2]，そして2013年10月に金原出版より改訂版『膵癌診療ガイドライン2013[3]』が出版された．

ガイドライン2009より2013の変更点について簡単に概説する．

2 科学的根拠に基づく膵癌診療ガイドライン

2006年3月に初版の『科学的根拠に基づく膵癌診療ガイドライン』[1]が出版され，2009年9月に第2版[2]が出版された．4年後の2013年春をめどに改訂を目指していた．しかし，JASPAC-01（切除膵癌に対する術後補助療法におけるS-1とゲムシタビン塩酸塩の前向き臨床試験）の結果[4]が2013年1月のASCO GIで発表されることがわかり，しかも，重要な結果であることが予想された．そのため，わが国よりの前向き臨床試験であるJASPAC-01の結果までは改訂に含むこととし，約半年，刊行を遅らせ，2013年10月に発刊した．

3 科学的根拠に基づく膵癌診療ガイドライン2013

2013年版は2006年，2009年版と同様，『Mindsガイドライン作成の手引き2007』[5]に従い，evidence based medicine（EBM）に基づくものとなっている．今回は改訂委員会は田中雅夫委員長，船越顕博副委員長から，委員長が山口幸二，副委員長が奥坂拓志副委員長に替わり，委員は約8割が入れ替わり，患者代表者（PanCAN JAPANの眞島喜幸氏）にも作成段階より参加していただいた．今回は社会的要求に鑑み，作成者のCOIを“本ガイドラインについて”前書きに記載した．

ステント部門が新設され，JA尾道総合病院の花田敬士先生にチーフをお願いした．分野はステント療法が追加され，5分野から6分野となった．また，分野の順番が1）診断法，2）化学療法，3）放射線療法，4）外科的治療法，5）補助療法から，1）診断法，2）外科的治療法，3）補助療法，4）放射線療法，5）化学療法，

Koji YAMAGUCHI：Alterations of clinical guidelines of pancreatic cancer from 2009 to 2013
*藤元総合病院［〒885-0055 宮崎県都城市早鈴町17街区1号］

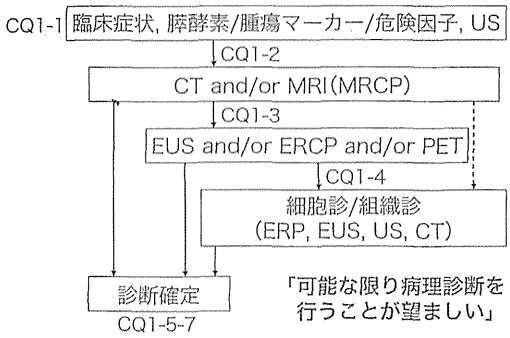

図1　膵癌診断のアルゴリズム2013

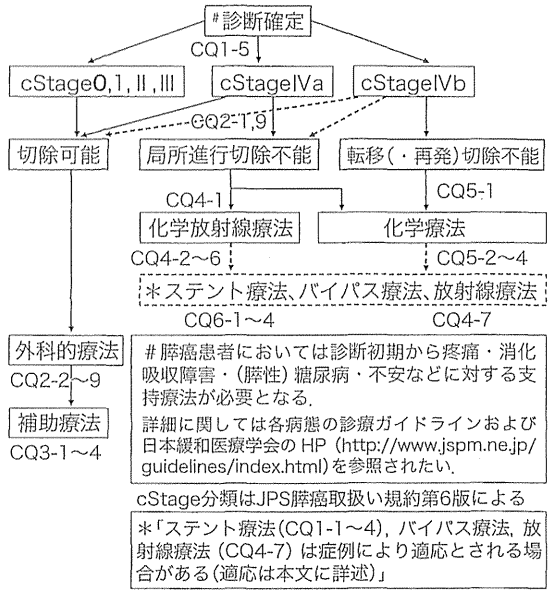

図2　膵癌治療のアルゴリズム2013

6)ステント療法に変更となった.

採用論文数は2006年，2009年，2013年で288，443，629と大きく増加した．CQは2006年版，2009年版，2013年版で22，25，35と増加し，推奨も31，39，57と大きく増加した．しかし,推奨度をみるとA:B:C(C1, C2):Dは4:12:5:9，4:18:17 (16，1):0，8:26:23 (22，1):0で相変わらずAは少なく，B，Cが依然として多い．膵癌に対する科学的エビデンスの高い論文が少ない状況は変わりないためと思われる．推奨，推奨度，明日への提言，構造化抄録のCD-ROMなどは過去2版と同様に作成した．ガイドライン2013では新たな試みとして，モバイル端末でCQ，推奨，推奨度，明日への提言のみをダウンロードできるようにし，利用しやすいようにした．6カ月間で1,500回ほどのダウンロード数となり，ガイドラインが使いやすくなっていると思われる．出版前のガイドラインの外部評価では，2009年版はAGREE Iで行ったが，今回は最新版のAGREE IIを用いて評価し，その内容を巻末に掲載した.

1. 診断(図1)と治療(図2)のアルゴリズム

診断のアルゴリズム(図1)はCT and/or MRI (MRCP)より「細胞診・組織診」に点線での流れが追加された．また，「可能な限り病理診断を行うことが望ましい」の文言が追加された．治療のアルゴリズム(図2)ではcStageの次に「切除可能」，「局所進行切除不能」，「転移(・再発)切除不能」が挿入された．「borderline resectable」を「切除可能」と「局所進行切除不能」の間に入れてはどうかとの意見があったが，まだわが国での定義も決まっておらず，時期尚早との判断で次回の検討課題として残された．また，「ステント療法，バイパス療法，放射線療法」の支持療法が追加された．膵癌と診断された時点より,疼痛・消化吸収障害・(膵性)糖尿病・不安などに対する支持療法が必要であることを，「診断確定」に＊で付記し，膵癌患者のすべてに関わる問題とした．Best supportive care(BSC)は，患者にとってやや印象がよくないとの意見で，今回のガイドラインの治療アルゴリズムより削除された．支持療法の詳細に関しては「各病態の診療ガイドラインおよび日本緩和医療学会のホームページ〈http://www.jspm.ne.jp/guidelines/index.html〉を参照された

表1

1診断（チーフ：清水先生）	
CQ1-1	膵癌のリスクファクターとは何か？（清水先生）
CQ1-2	膵癌の発見はどのようにしたらよいか。（中泉先生）
CQ1-3	膵癌を疑った場合，次に行うべき検査は何か？（糸井先生）
CQ1-4	膵癌の診断を確定するための次のステップはどうするか？（水野先生）
CQ1-5	膵癌の病期診断はどのように決定するか？（羽鳥先生）
CQ1-6	Borderline resectable膵癌の診断：本邦におけるBorderline resectableとは？（山上先生）
CQ1-7	長期予後が期待できる早期の膵癌を診断するにはどうするか？（花田先生）

表2　外科切除可能膵癌

2外科的療法（チーフ：山口）	
CQ2-1	Stage IVa膵癌に対する手術的切除療法の意義はあるか？（江川先生）
CQ2-2	腹腔洗浄細胞診陽性症例の切除の意義はあるか？（藤井先生）
CQ2-3	膵頭部癌に対しての膵頭十二指腸切除において胃（全胃あるいは亜全胃）を温存する意義はあるか？（山口）
CQ2-4	膵癌に対する門脈合併切除は予後を改善するか？（藤井先生）
CQ2-5	膵癌に対して拡大リンパ節・神経叢郭清の意義はあるか？（横山先生）
CQ2-6	（開腹後）非切除例での予防的バイパス療法は予後を改善するか？（山口）
CQ2-7	膵癌に対する内視鏡的手術の意義は？（遠藤先生）
CQ2-8	膵癌では手術例数の多い施設で治療を受けるのがよいか？（江川先生）
CQ2-9	Borderline resectable膵癌の治療：本邦における外科的切除の意義は？（山上先生）

い.」という文章を脚注に挿入した.

2. 診断部門（表1）

診断部門ではCQ1-6 “Borderline resectable pancreatic cancer”とCQ1-7 “長期生存が期待できる早期の膵癌”が新たに取り上げられた. CQ1-6のBorderline resectable pancreatic cancerはわが国では定義が定まっていないため，アメリカのNCCNガイドラインでの定義を示し，“膵癌の局所浸潤により外科的切除をしても高率に癌が遺残し（R1もしくはR2），切除による生存期間延長効果を得ることができないものとなる可能性がある”のその概念の紹介にとどめている. また，随伴性膵炎と癌浸潤との術前画像診断での鑑別診断の難しさも述べている.

CQ1-7の早期の膵癌の診断として，“主膵管の拡張，嚢胞の間接所見で引き続き行うMRCP，EUSの重要性と前記の画像診断所見で限局性膵管狭窄が認められた場合，ERCPと膵液細胞診を繰り返し行うこと”の重要性を強調している.

CQ1-1ではリスクファクターで合併疾患として膵嚢胞が追加された. CQ1-2の膵癌の発見で“血中膵酵素は膵疾患診断に重要だが，膵癌に特異的ではない”でグレードC1であったが，今回は“血中膵酵素測定は膵癌に特異的ではないが，早期診断に有用性が認められている”としてグレードBが付いた. “臨床症状，膵酵素/腫瘍マーカー/危険因子，USで膵癌が疑われた場合，CTを初めとする検査を行う”ことがグレードAで推奨されていたが，今回はグレードは付記されていない. CQ1-3膵癌を疑った時の画像診断としてMRI（MRCP）に（造影および3テスラ以上が望ましい）が追記されている.

3. 外科的治療部門（表2）

外科的治療法はCQ4であったが，今回は膵癌の診断，外科切除，補助療法が一番期待される膵癌治療の流れであろうとのことで，

CQ2となっている．CQ2-2 “腹水洗浄細胞診の意義”，CQ2-7 “内視鏡的手術”と2-9 “Borderline resectable pancreatic cancerの外科切除の意義”が追加された．CQ2-2 “腹腔洗浄細胞診陽性症例の切除の意義はあるか？”は推奨“腹腔洗浄細胞診陽性の膵癌に対しての膵切除を行うべきか否かは明らかではない．今後，臨床試験や研究の蓄積によって明らかにされるべきである(グレードC1)．”となっている．CQ2-7 “膵癌に対する内視鏡的手術の意義は？”は推奨“膵癌に対する内視鏡的手術は症例を選べば安全に施行可能である．長期遠隔成績を向上させるか否かについてはhigh volume centerでの症例の蓄積により明らかにされるべきである(グレードC1)．”となっている．CQ2-9 “Borderline resectable膵癌の治療：わが国における外科的切除の意義は？”は推奨“Borderline resectable膵癌に対して補助(術前)治療を行うことで，外科的切除の治療成績が改善するかについては今後の臨床試験や研究で明らかにされるべきである(グレードC1)．”となっている．

4. 補助療法部門(表3)

CQは変わっていないが，内容は大きく変わった．2009年版CQ5-2 “術中切除面への放射線療法”の推奨が“術中放射線療法の有効性を支持する十分なエビデンスはいまだに示されておらず，これが予後を改善させるか否かについては，今後の臨床試験や研究の蓄積によって明らかにされるべきである(グレードC1)．”から，2013年版CQ3-2で国立がん研究センター東病院を中心とした前向き臨床試験の結果を受けて，“膵癌に対する術中放射線療法の有用性は明らかではない．日本で行われたランダム化比較試験では，術中放射線単独の効果は認められなかった(グレードC2)．”に推奨が変更された．

表3　外科切除可能膵癌

3補助療法（チーフ：古瀬先生）	
CQ3-1	膵癌に対する術前治療(①化学放射線療法および，②化学療法)は推奨されるか？（大東先生）
CQ3-2	膵癌の術中放射線療法は推奨されるか？（中郡先生）
CQ3-3	膵癌の術後化学放射線療法は推奨されるか？（菅野先生(中村先生のサポート)）
CQ3-4	術後補助化学療法を行うことは推奨されるか？（上坂先生）

術後化学療法は2009年版CQ5-4 “国際的に十分なコンセンサスが得られた術後補助療法のレジメンは確立していないが，ゲムシタビン塩酸塩による術後補助化学療法は有用性，安全性の点で比較的良好な成績を示しており推奨される．”でゲムシタビン塩酸塩がグレードBで推奨されていたが，JASPAC01の結果を受けて，2013年版CQ3-4で“術後補助化学療法は切除単独に比べ良好な治療成績を示しており，実施することが勧められる(グレードA)．術後補助療法のレジメンはS-1単剤療法が推奨され(グレードA)，S-1に対する忍容性が低い症例などではゲムシタビン塩酸塩単独療法が勧められる(グレードB)．”とグレードAはゲムシタビン塩酸塩よりS-1単剤療法に変更された．

5. 放射線療法部門(表4)

新たにQ4-1，CQ4-4，CQ4-7が追加された．CQ4-1で“局所進行切除不能膵癌に対する一次治療としては，化学放射線療法または化学療法単独による治療が推奨される(グレードA)（化学放射線療法，化学療法の具体的な治療レジメンは，CQ4-2，CQ5-2において推奨する)．”となっている．CQ4-4として“局所進行切除不能膵癌に対し，化学放射線療法前の導入化学療法の意義はあるか？”が追加さ

表4　局所進行切除不能膵癌

1．局所進行切除不能膵癌に対して一次治療として化学放射線療法を行う場合(チーフ：伊藤(芳)先生)

4 化学放射線療法（放射線療法：チーフ伊藤（芳）先生）

CQ4-1　局所進行切除不能膵癌に対して推奨される一次療法は何か？（伊藤(芳)先生）
CQ4-2　推奨される化学放射線療法は何か？（澁谷先生）
CQ4-3　局所進行切除不能膵癌に対する外部放射線治療ではどのような臨床標的体積を設定するのがよいか？（中村先生）
CQ4-4　局所進行切除不能膵癌に対し、化学放射線療法前の導入化学療法の意義はあるか？（大栗先生）
CQ4-5　局所進行切除不能膵癌に対し術中放射線療法の効果はあるか？（大栗先生）
CQ4-6　放射線療法は局所進行非切除膵癌のQOLを改善するか？（永倉先生）

2．局所進行切除不能膵癌に対して一次治療として化学療法を行う場合(一次治療として化学放射線療法を行う場合の「導入化学療法」を除く)，（チーフ：奥坂先生）CQ5-2, 3, 4を参照

れ，“局所進行切除不能膵癌に対し化学放射線療法前に導入化学療法を行うことで，同時化学放射線療法を施行するメリットの高い症例群が選別され，選別例では良好な治療成績が報告されている点から意義があり，治療選択肢として考慮されてもよい(グレードC1)．”となっている．CQ4-7の“膵癌骨転移に対する放射線療法”が取り上げられ，“骨転移による疼痛緩和に放射線療法は有用である(グレードA)．”で推奨されている(表4)．

2009年版CQ3-1で“局所進行切除不能膵癌に対し化学放射線療法は有効か？”に対して，推奨“局所進行切除不能膵癌に対する5-FU併用化学放射線療法は有効な治療法であり，治療選択肢の一つとして推奨される(グレードB)．”であったが，CQ4-1 “局所進行切除不能膵癌に対して推奨される一次治療は何か？”に対して推奨“局所進行切除不能膵癌に対する一次治療としては，化学放射線療法または化学療法単独による治療が推奨される(グレードA)（化学放射線療法，化学療法の具体的な治療レジメンは，CQ4-2，CQ5-2において推奨する)．”となっている．

2009年版CQ3-2で“局所進行切除不能膵癌に対して，化学放射線療法を行う場合の標準的な併用化学療法は5-FUである(グレードB)．ゲムシタビン塩酸塩との併用については積極的に推奨するだけの科学的根拠が十分でないものの，その有用性を示唆する報告もあり，安全性が確認されたレジメンにおいて十分な説明を行い同意を得たうえで実施することは，選択肢の一つとして考慮されてもよい(グレードC1)．”となっていたが，CQ4-2 “局所進行切除不能膵癌に対して推奨される化学放射線療法は何か？”に対して，推奨“局所進行切除不能膵癌に対して，放射線療法を行う場合には，フッ化ピリミジン系抗がん薬またはゲムシタビン塩酸塩との併用が推奨される(グレードB)．放射線療法については，3次元治療計画を行い，腫瘍に対する正確な照射と正常臓器への線量低減を図ることが推奨される．”となっている．

2013年版CQ4-6は2009年版CQ3-5が対応し，“放射線療法は切除不能膵癌のQOLを改善するか？”であったが，CQが“放射線療法は局所進行切除不能膵癌のQOLを改善するか？”となり，推奨も“切除不能膵癌のQOL改善には，放射線療法(グレードC1)や化学放射線療法(グレードB)が勧められる．”から“局所進行切除不能膵癌のQOL改善には，化

学放射線療法(グレードB)や放射線療法(グレードC1)が勧められる."となっている.

6. 化学療法部門(表5)

CQは変わっていないが,内容は大きく変わった."切除不能膵癌の化学療法の一次化学療法"の推奨が2009年版GEM単剤(グレードA)から2013年版ではGEM単剤,GEM+エルロチニブ,またはS-1単剤が推奨度Aで推奨された.これにはわが国を中心に行われた前向き臨床試験であるGESTの結果が大きく影響している.当時,保健収載されていなかったFOLFIRINOXや現在も保健収載になっていないGEM+nab-パクリタキセルなども解説文の中で取り上げられている.さらに,2014年7月9日に日本膵臓学会HP上でCQ5-2-1とCQ5-2-2に分けて改訂された.CQ5-2-1 "遠隔転移を有する膵癌に対して推奨される一次化学療法は何か?"に対して推奨はFOLFIRINOXの保健収載をふまえて,推奨"遠隔転移を有する膵癌に対する一次化学療法としては,FOLFIRINOX療法,ゲムシタビン塩酸塩単剤治療,ゲムシタビン塩酸塩+エルロチニブ塩酸塩併用治療,またはS-1単剤治療が推奨される(グレードA).ただし,FOLFIRINOX療法は,化学療法に十分な経験のある医師のもとで,全身状態(PS),年齢,骨髄機能,黄疸・下痢の有無,UGT1A1の遺伝子多型などを考慮し,実施に際しては,緊急時にも適切な対応ができるよう,有害事象に対する十分な観察と対策が必要である."となっている.また,CQ5-2-2 "局所進行切除不能膵癌に対して推奨される一次化学療法は何か?"に対して推奨は"局所進行切除不能膵癌に対する一次化学療法として,ゲムシタビン塩酸塩単剤治療,またはS-1単剤治療が推奨される(グレードA)."となっている.

表5 遠隔転移・再発切除不能膵癌

5 化学療法(チーフ:奥坂先生)
CQ5-1 遠隔転移を有する膵癌患者に対して化学療法は推奨されるか?(木原先生)
CQ5-2 局所進行切除不能膵癌・転移性病変を有する膵癌に対して推奨される一次化学療法は何か?(木原先生)
CQ5-3 切除不能膵癌に対して推奨される化学療法の投与期間は何か?(伊藤(鉄)先生)
CQ5-4 切除不能膵癌に対して二次化学治療は推奨されるか?(古瀬先生)
4 放射線療法(チーフ:伊藤(芳)先生)
CQ4-7 膵癌骨転移に対する放射線療法は有用か?(澁谷先生(放射線療法))
6 ステント療法(チーフ:花田先生)
ステント療法をどう考えるか?(CQ6-1よりCQ6-4を参照とする)

2009年版CQ2-4の二次化学療法については"わが国においては保険適応内で十分な科学的根拠を有する二次化学療法薬はないが有用性を示唆する報告もあり,また,海外においてはランダム化比較試験により有用性を示した二次化学療法も最近報告されている.PSの良好な患者に対して十分な説明と同意を得たうえで二次化学療法を実施することは選択肢の一つとして考慮してもよい(グレードC1)."より2013年版CQ5-4 "海外における二次治療のランダム化比較試験により,支持療法に比べ化学療法の有用性が示されており,二次化学療法の実施が推奨される(グレードB).二次化学療法のレジメンは一次治療に応じて,S-1もしくはゲムシタビン塩酸塩を選択する(グレードC1)."とグレードが上がっている.さらに,2014年7月9日に日本膵臓学会HP上でCQ5-4 "切除不能膵癌に対して二次化学療法は推奨されるか?"に対して,推奨は"海外における二次治療のランダム化比較試験により,支持療法に比べ化学療